Photoexcitation dynamics in polythiophene/fullerene blends for photovoltaic applications

C.-X. Sheng[1,2] , T. Basel[1], B. Pandit[1] and Z. V. Vardeny[1]*

[1] Department of Physics & Astronomy, University of Utah Salt Lake City, Utah 84112, USA

[2] School of Electronic and Optical Engineering,
Nanjing University of Science & Technology, Nanjing 210094, China

Abstract

We used the transient and steady state photomodulation spectroscopies for studying the photoexcitations dynamics in blends of regio-regular poly(3-hexylthiophene) (RR-P3HT) and fullerene in a broad spectral range from 0.15 to 2.25 eV. We found that both localized polarons and singlet excitons are instantaneously photogenerated in the blends. However the photogeneration process of delocalized polarons which contribute to the photocurrent proceeds in two steps: first, within a couple of ps the excitons generated in the polymer domains populate the charge transfer complex states at the RR-P3HT/fullerene interfaces; this is followed by the charge transfer ionization into delocalized charge polarons in the polymer and fullerene constituents within ~20 ps. In contrast, the localized polaron dynamics are unrelated with the excitons and delocalized polarons dynamics. We also report on the occurrence of ultrafast quantum interference anti-resonances between photoinduced infrared-active vibrations and the delocalized polaron band in the blends, which shows the delocalization character of the photogenerated charges that contribute to the photocurrent.

To whom correspondence should be addressed; e-mail: val@physics.utah.edu

1. Introduction

Organic photovoltaic (OPV) solar cells based on blends of π-conjugated polymers with fullerene molecules have attracted widespread interests in both academic and commercial communities in recent years. One of the most studied bulk heterojunction (BHJ) organic photovoltaic materials is the blend of regio-regular poly (3-hexylthiophene) (RR-P3HT) and [6,6]-phenyl-C_{61}-butyric acid methyl ester (PCBM), which is often considered as a "model BHJ system" [1, 2]. The P3HT/PCBM blend films are characterized by charge photogeneration with high efficiency, and phase separated fullerene and polymer networks that facilitate charge transport. Consequently high power conversion efficiencies up to ~4.5% can be obtained in solar cells based on RR-P3HT/PCBM BHJ photovoltaic devices [3, 4]. Numerous steady-state and time-resolved spectroscopic studies have been conducted in pristine P3HT and P3HT/PCBM blend in order to understand the properties and evolution of neutral and charged photoexcitations; but many aspects of the photophysics still remain unclear [5-20]. One of the reasons for this is the additional complications that arise due to the strong chain-chain interaction in the self-organized π-stacked two-dimensional (2D) lamellae of the polymer domains in the films [16]. Therefore, unlike many other π-conjugated polymers in which photoexcitations are usually localized on almost isolated polymer chains, it has been shown that in RR-P3HT films both neutral and charge photoexcitations are delocalized within the 2D lamellae along the π-stacking direction [16-19].

In this work we used both transient and continuous wave (cw) photomodulation (PM) spectroscopies for studying the photoexcitations dynamics in pristine RR-P3HT and RR-P3HT/PCBM blends in a unique broad spectral range from 0.15 to 2.25 eV. In the blend we show that both localized polarons (LP) and singlet excitons are instantaneously photogenerated. However the photogeneration process of delocalized polarons (DP) which contribute to the photocurrent in OPV cells proceeds in two steps: first, within a couple of ps the excitons generated in the polymer domains are

trapped in the charge transfer complex (CTC) at the RR-P3HT/fullerene interfaces; this is followed by the CTC ionization into DP in the polymer and fullerene constituents within ~20 ps, which can readily contribute to the photocurrent in the film. In contrast, we found that the localized polaron density is unrelated with the excitons and DP dynamics. We also measured in the blend photoinduced ultrafast quantum interference anti-resonances between the photoinduced infrared-active vibrations and the DB band in the near-IR spectral range, which shows the delocalization character of the photogenerated mobile charges.

2. Experimental

The femtosecond (fs) two-color pump-probe correlation technique was used for measuring the transient photoexcitation response dynamics in the fs to ns time domain. Two fs Ti:sapphire laser systems were utilized to cover the broad probe photon energy; (i) a low power (energy/pulse ~0.1 nJ) high repetition rate (~80 MHz) [21] laser system for the mid-IR spectral range; and (ii) a high power (energy/pulse ~10 μJ) low repetition rate (~1 kHz) laser system for the near-IR/visible spectral range [21]. For both laser systems the excitation photon energy, $\hbar\omega$(pump) was set at ~3.1 eV using a second harmonic generation crystal.

For system (i) in the mid-IR range both signal and idler output of an optical parametric oscillator (Tsunami, Opal, Spectra Physics) were used respectively as probe beams in the spectral interval $\hbar\omega$(probe) ranging from 0.55 to 1.05 eV. In addition a difference frequency set up based on a nonlinear optical crystal was used to extend the probe spectral range from ~0.15 to ~0.43 eV. For system (ii) white light super-continuum was generated having $\hbar\omega$(probe) in the range from 1.2 to 2.7 eV. The transient PM signal, $\Delta T/T$(t) is the fractional change, ΔT in transmission, T, which is negative for PA, and positive for photobleaching (PB). The transient PM spectra from the two laser systems were normalized to each other in the near-IR/visible spectral range, where $\hbar\omega$(probe) from the low power laser system was doubled. The pump and

probe beams were carefully adjusted to get complete spatial overlap on the film, which was kept under dynamic vacuum. In addition, the pump/probe 'beam-walk' caused by the translation stage was carefully monitored, and the transient PM response was adjusted by the 'beam-walk' measured response [21].

The steady state PM spectrum was obtained using a standard cw setup [8]. For excitation we used a cw Ar^+ laser pump beam at $\hbar\omega_L$=2.5 eV that was modulated at frequency *f*; and an incandescent tungsten/halogen lamp as the probe. The PM spectrum was measured using a lock-in amplifier referenced at *f*, a monochromator, and various combinations of gratings, filters, and solid-state photodetectors spanning the spectral range 0.3 <$\hbar\omega$(probe)< 2.3 eV. This setup was also used for measuring the photoluminescence spectrum. To cover the range $\hbar\omega$(probe)<0.3 eV we used a FTIR spectrometer. The Ar^+ laser beam was modulated with a shutter, and the transmission spectrum of the film was measured with the excitation beam on and off. About 5000 scans for *T*(off) and *T*(on) (where *T*(on) and *T*(off) is the obtained transmission spectrum with the excitation laser beam on and off, respectively) were recorded, and subsequently $\Delta T/T$ spectrum was calculated using the relation [*T*(on)-*T*(off)]/T(off). The PM spectra obtained with both set ups were normalized to each other in the $\hbar\omega$(probe) range of 0.3-0.4 eV.

RR-P3HT and PCBM were purchased from ADS Inc.; they were used without further purification. The mixing ratio of the RR-P3HT/PCBM blend was 1.2:1 by weight; this ratio was chosen since it gives the highest power conversion efficiency in OPV cells application [4]. The films were drop cast onto CaF_2 substrates from dilute toluene solution. The films preparation and annealing (for the blend only) were done in nitrogen atmosphere in a glovebox.

The bulk heterojunction organic photovoltaic devices were fabricated using RR-P3HT (8mg/ml)/PCBM solution of 1.2:1 mass ratio in toluene. The devices were comprised of thin film of indium tin oxide (ITO) anode; PEDOT:PSS hole transport layer; layer of spin-coated RR-P3HT/PCBM blend; and capped with Ca/Al cathode [22]. The ITO coated glass with low sheet resistance (~10Ω/□) was purchased from Delta Technologies. The substrate was cleaned with acetone, 2% micro-90 cleaning solution, de-ionized water and methanol. A thin hole transport layer (50 nm) of a mixture of poly(3,4-ethylenedioxythiophene) and poly(styrenesulfonate) (PEDOTT: PSS) was spin coated over the substrate and subsequently dried for half an hour at 100˚C in a glove-box. The P3HT/PCBM solution was spin coated on the substrate at 650 rpm and annealed at 150˚C for half an hour. The device fabrication was completed by thermally evaporated a 20 nm Ca followed by an 80 nm Al. Finally the completed device was encapsulated with a cover glass using Norland 6106 UV-curable optical adhesive to protect the device from oxygen and water in the air. The device I-V characteristics under sun-like illumination was measured using a Keithley 236 Source-Measure unit. The light source was a Xenon lamp with an AM1.5 filter of which intensity was calibrated to 100 mW/cm^2 using a silicon PV cell that was pre-calibrated at NREL.

3. Results and discussion

Fig. 1(a) shows the cw PM spectrum of a RR-P3HT/PCBM film at 80 K; it contains four PA bands. Two PA bands (DP_1 at 0.09 eV and DP_2 at 1.8 eV) are due to 2D delocalized polarons (DP) in the RR-P3HT ordered domains (lamellar structure with enhanced interchain coupling [16]); whereas the other two PA bands (P_1 at 0.35 eV and P_2 at 1.25 eV) are due to localized intrachain polarons (LP) in the disordered P3HT regions of the film [8, 16]. An interaction model depicted in Fig. 1(b) shows that the interchain interaction in the RR-P3HT lamellae splits the intrachain DP levels, resulting in energy shift of the DP allowed optically transitions [16] respect to those of LP. This may explain the reason that DP_1 is red shifted respect to P_1, whereas DP_2 is

blue shifted respect to P_2 [16]. The sharp dips (anti-resonances) superimposed on the DP_1 band (shown more clearly in Fig. 1(a) inset) are due to photoinduced infrared-active vibrations (IRAVs), which usually appear as PA lines in less ordered films such as blend of 2-methoxy-5-(2'-ethylhexyloxy) poly(phenylene-vinylene) (MEH-PPV)/C_{60} [23]. The cw photoinduced Fano-type anti-resonances (AR) have been explained using non adiabatic amplitude mode model and charge density wave conductivity band, which indicates the existence of a continuum band in RR-P3HT/PCBM blend films [24].

Although the DP excitation in the lamellae of RR-P3HT/PCBM blend has been recognized for playing an important role in the optoelectronic response of organic devices [9], the mechanism for the DP photogeneration in RR-P3HT/PCBM is still debated. One model proposes that the exciton photoexcitation in the polymer constituent dissociates within hundreds of femtoseconds [9, 24], while the electron transfers to the PCBM molecule, and the remaining hole resides in the polymer chain. However whether the hole excitation in the polymer domain is LP or DP type is still unclear. It has been also suggested [5] that the ultrafast charge separation in polymer/fullerene blends occurs before localization of the primary excitation to form a bound exciton. In contrast, evidence for the existence of a charge transfer complex (CTC) state in the interfaces between the polymer and PCBM domains, and its role as an intermediate state in the DP photogeneration have been also reported [1, 10, 26, 27]. Several techniques such as electro-absorption, below-gap pump excitation PM, as well as photoluminescence [10, 26, 27] have been applied to study the CTC in polymer/fullerene blends. For further studying the CTC role in the charge photogeneration in the blend we need to investigate the photoexcitation ultrafast dynamics.

Fig. 2(a) and Fig. 3 present the transient PM spectra of RR-P3HT/PCBM blend film measured at t = 0 ps and t = 50 ps, from 0.13 eV to 1 eV and from 1.25 eV to 2.25 eV,

respectively. The t=0 ps PM spectrum contain five PA bands: PA_1 at ~0.95 eV, P_1 at ~0.35 eV, and DP_1 band below 0.3 eV (seen in Fig. 2), and P_2 at ~1.4 eV and DP_2 at 1.9 eV (seen in Fig. 3), respectively. PA_1 band was previously assigned to optical transitions related to the photogenerated singlet intrachain excitons [8, 10]; it is seen that it decays within about 20 ps (Fig. 2(b)). Consequently the transient PM spectrum at t = 50 ps contains only four bands, namely DP_1, P_1, P_2 and DP_2 (in increasing photon energy order); consistent with the cw PM spectrum (Fig.1 (a)). However, the relative intensities of the PA bands are very different in the cw and transient spectra. This indicates that the various PA bands have different dynamics.

PA_1 dynamics cannot be fit using a single exponential decay; a better fit is achieved using two exponentials, namely $A_1\exp(-t/\tau_1)+A_2\exp(-t/\tau_2)$ with $\tau_1 = 2.6$ ps, $\tau_2 = 22$ ps, respectively. The relatively small τ_1 value is surprising because the exciton dissociation was expected to be on a time scale less than 1 ps [9, 24]. We thus conclude that the delayed dynamics involves exciton diffusion to the donor-acceptor (D-A) interfaces. In contrast, P_1 dynamics (Fig.2(c)) reveals that these polarons are created instantaneously along with the excitons [14]; and in addition P_1 does not grow at the expense of PA_1 decay. Also P_1 remains constant after about 150 ps (Fig. 3(b)). Moreover PA_1 (Fig. 2(d)) and P_1 dynamics do not change with the excitation intensities. We thus conclude that the photogenerated LP (P_1) and exciton (PA_1) species are uncorrelated. The branching ratio, η of photogenerated polarons/excitons has been estimated from the relative intensity ratio P_1/PA_1 [i.e. integrated area under each respective PA band]. For this we used the low intensity laser system in order to avoid the complex recombination processes typical of high intensity laser systems [34]; we thus estimated η~80% at t = 0 ps. This indicates that the initial LP population is relatively higher in the blend compared to the pristine RR-P3HT film (η=30% [14]), which could be explained as due to larger disorder and impurity density in the blend. In support for this conclusion we note that after annealing the same film at 150^{o}C for 30 minutes, η decreases to ~30% at t = 0 ps (Fig. 2(a) inset).

We also note that the populations of the LP and excitons are unrelated in both pristine and annealed blend films. On the other hand DP_1 at 0.25 eV grows exponentially, with a time constant τ=19 ps (Fig. 2(b)), which is very close to the τ_2 time constant of PA_1 decay. This shows that DP_1 rises on the expense of PA_1 decay, and this is compelling evidence that the delocalized polarons are in fact created once the excitons decay when arriving to the D-A interfaces. I-V characteristic under sun illumination of a device fabricated using RR-P3HT/PCBM solution of 1.2:1 mass ratio in toluene is shown in Fig. 2(e). The device performance is fairly good with estimated power conversion efficiency of 2.1% and fill factor of 50%. This indicates that the polymer lamellar structure, and the D-A phase separation in the RR-P3HT/PCBM films used for our spectroscopic studies are definitely in place.

In addition the PM spectrum in the visible/near-IR range (Fig. 3) shows a rise of DP_2 band in the ps range. We note that its dynamics was probed at 1.55 eV (within the DP_2 spectral range) using the low intensity laser system to avoid bimolecular recombination. We can clearly see that the 'rise dynamics' of DP_2 and DP_1 measured using the same laser system are identical (Fig. 3 inset), which gives another evidence for the generation of DP excitations on the expense of the excitons decay [7, 28]. The PM also shows a spectral feature associated with photoinduced electro-absorption modulation with phonon sidebands at ~1.9, 2.05, and 2.23 eV, respectively [14]; which indicates that most photoexcitations in the blends are in fact charged, and hence form photoinduced internal electric fields.

The most striking consequence of the DP photogeneration in the ps time domain is the quantum interference AR between photoinduced infrared vibrations and DP_1 band, as shown in Fig. 4(a). The inset of Fig. 4(a) shows the cw PM spectrum of the blend film for comparison. The dips at ~0.18 eV and ~0.16 eV in the transient PM spectrum clearly appear after ~200 ps with similar spectrum as that obtained in cw conditions. The AR dips are caused by the overlap between the discrete vibrational lines and DP_1

continuum band [24]. The complex AR structure in the cw PM spectrum was calculated before using the non-adiabatic version of the amplitude mode (AM) model coupled to charge density wave of a conductivity continuum band; this led to the identification of a continuum band in ordered polymer films such as RR-P3HT [8, 24].

The AM model has had spectacular success in explaining the resonant Raman scattering (RRS) dispersion in PCPs, as well as photoinduced and doping induced IRAVs. Because the Raman vibrational energies are much smaller than the optical gap, and also their corresponding IRAV frequencies are much smaller than the energy of photoinduced and doping induced electronic bands, many applications of the AM model were based on the adiabatic approximation [29, 30]. However this approximation does not hold true in the case of RR-P3HT/PCBM blends here since the IR-active lines overlap with the electronic transition of delocalized polarons (see energy diagram of Fig.1). Therefore, both vibronic and electronic excitations, as well as their quantum interference have to be taken into account to evaluate the conductivity $\sigma(\omega)$ (hence the absorption spectrum since imaginary ($\sigma(\omega) \approx \alpha(\omega)$).

The conductivity spectrum $\sigma(\omega)$ consists of two parts [31, 32]; one is determined by the most strongly coupled phonons in the non-adiabatic limit; the other is related to the system response in the absence of phonons. In the charge-density wave approximation, the sharp features in $\sigma(\omega)$ are given by the relation [24]:

$$\sigma(\omega) \approx \frac{1 + D_0(\omega)[1 - \alpha_p]}{1 + D_0(\omega)[1 + C - \alpha_p]} \qquad (1)$$

where C is a constant that presents a smooth electronic response; α_p is defined as polaron-vibrational 'pinning parameter' for the trapped polaron excitation; and $D_0(\omega)$ is the 'bare' phonon propagator. The latter is given [29] by the relation: $D_0(\omega) = \Sigma_n d_{0,n}(\omega)$, and $d_{0,n}(\omega) = \lambda_n/\lambda\{(\omega_n^0)^2/[\omega^2-(\omega_n^0)^2-i\delta_n]\}$, where ω_n^0, δ_n and λ_n are the

'bare' phonon frequencies, their natural linewidth (inverse lifetime) and electron-phonon (e-p) coupling constant, respectively; and $\Sigma\lambda_n = \lambda$, which is the total e-p coupling.

The poles of Eq. (1), which can be found from the relation: $D_0(\omega) = -(1-\alpha_p + C)^{-1}$ produce peaks (or IRAV's) in $\sigma(\omega)$. We have previously used the IRAV's, which appear as positive absorption lines to identify the charge state of photoexcitations in the ps PM spectra of less ordered PCPs' films [33]. In contrast the zeros in Eq. (1), which can be found by the relation: $D_0(\omega) = -(1-\alpha_p)^{-1}$ produce indentations (or ARs) in $\sigma(\omega)$. Eq. (1) was used before to successfully fit the cw AR features indicating the existence of a continuum band in RR-P3HT/PCBM blend films [24]. Therefore the obtained transient AR features in the ps transient PM spectrum provides direct evidence that the photogenerated DP species in the blend are *free charges*, since they form a continuum absorption band that is coupled to IRAVs.

The transient dynamics of the PM spectrum near the AR features are shown in more detail in Fig. 4(b); dramatic different behavior for close-by energies is clearly seen. It is interesting to note that the PA dynamics at 0.18 eV and 0.16 eV are very different, although they both belong to the AR features. Apparently the anti-resonance effect is stronger at 0.18 eV, which is probably caused by the stronger e-p coupling of this mode (related to the C=C stretching vibration) [19, 30].

From the cw PM spectrum reported previously [8, 16] we know that DP excitations are also photogenerated in pristine RR-P3HT films. It is therefore interesting to investigate the ultrafast PM spectrum and dynamics of pristine RR-P3HT film in mid-IR in comparison with the cw PM spectrum; this is shown in Fig. 5. As is clearly seen the transient and cw PM spectra are very different from each other. Whereas the ps transient PM spectrum is dominated by the LP excitations with PA at 0.35 eV, the cw PM spectrum is dominated by the DP excitations with PA at ~ 0.1 eV. In addition

Fig. 5 also shows that there are no photoinduced infrared vibrations related to the photogenerated LP excitations, indicating that these polarons are indeed localized. We therefore conclude that the DP excitations seen in cw PM spectrum of pristine RR-P3HT are generated at a later time, probably as a result of exciton ionization; in contrast the LP that are generated in the ps time domain decay via geminate recombination, and thus do not contribute to the generation of DP excitations directly.

4. Conclusions

In summary, we investigated the nature and ultrafast dynamics of the photoexcitations in RR-P3HT/PCBM blend that is utilized for photovoltaic applications. We found that localized polarons and singlet excitons are instantaneously photogenerated with almost equal probability in as prepared films; upon annealing the branching ratio, η between localized polarons and excitons decreases to about 30%. In contrast delocalized polarons that may contribute to the photocurrent are generated at the expense of excitons within ~20 ps, but do not correlate well with the generated localized polarons in the film. The high degree of phase separation in the blend results in the diffusion of excitons generated in the polymer domains towards the D-A interfaces, thereby forming an intermediate charge transfer exciton. We also identified the quantum interference anti-resonances between photoinduced infrared-active vibrations and delocalized polaron band in the ps time domain, indicating that the delocalized polarons form a continuum band in the blend film that indicates their ability to participate in charge transport.

Acknowledgements

We thank Drs. Tong and Yang for their help with the measurements. The work at the University of Utah was supported in part by the DOE Grant No. DE-FG02-04ER46109, and the MRSEC program at the University of Utah (grant No DMR11-21252). The work at Nanjing was supported in part by NSF China No. 61006014, National High Technology Research and Development Program of China

NO.2011AA050520. C.-X.S thanks the NUST Research Funding No.2011ZDJH23 and NUST ‘Zijin star’ project.

UU IR Author Manuscript

Reference:

[1] T. M. Clarke and J. R. Durrant, Chem. Rev. 110 (2010) 6736

[2] G. Dennler, M. C. Scharber, and C. J. Brabec, Adv. Mater. 21 (2009) 1223

[3] W. Ma, C. Y. Yang, X. Gong, K. Lee, and A. J. Heeger, Adv. Funct. Mater. 15 (2005) 1617.

[4] G. Li, V. Shrotriya, J. Huang, Y. Yao, T. Moriarty, K. Emery, and Y. Yang, Nat. Mater. 4 (2005) 864.

[5] N. Banerji, S. Cowan, E. Vauthey, and A. J. Heeger, J. Phys. Chem. C 115 (2011) 9726

[6]R. A. Marsh, J. M. Hodgkiss, S. Albert-Seifried and R. H. Friend, Nano Lett. 10 (2010) 923

[7] J. Guo, H. Ohkita, H. Benten and S. Ito, J. Am. Chem. Soc. 132 (2010) 6154

[8] X. Jiang, R. Osterbacha, O. Korovyanko, C.P. An, B. Horovitz, R.A.J. Janssen, and Z. V. Vardeny, Adv. Funct. Mater. 12 (2002) 587

[9] W. Hwang, D. Moses, and A.J. Heeger, J. Phys. Chem. C 112 (2008) 4350

[10] T. Drori, J. Holt, and Z.V. Vardeny, , Phys. Rev. B 82 (2010) 075207

[11] I. Montanari, A. F. Nogueira J. Nelson, and J.R. Durrant C. Winder, M. A. Loi, N. S. Sariciftci and C. Brabec, Appl. Phys. Lett. 81 (2002) 3001

[12] F. Paquin, G. Latini, M. Sakowicz, P. Karsenti, L. Wang, D. Beljonne, N. Stingelin, and C. Silva, Phys. Rev. Lett. 106 (2011) 197401

[13] A.J. Ferguson, N. Kopidakis, S.E. Shaheen, and G. Rumbles, J. Phys. Chem. C, 115 (2011) 23134

[14] C.-X. Sheng, M. Tong, S. Singh, and Z. V. Vardeny, Phys. Rev. B 75 (2007) 085206

[15] K. Kanemoto, M. Yasui, T. Higuchi, D. Kosumi, I. Akai, T. Karasawa, and H. Hashimoto, Phys. Rev. B 83 (2011) 205203

[16] R. Österbacka, C. P. An, X. M. Jiang, and Z. V. Vardeny, Science 287 (2000) 839

[17] J. Clark, C. Silva,R. H. Friend, and F. C. Spano, Phys. Rev. Lett. 98 (2007) 206406

[18] J. Clark, J-F Chang, F.C. Spano, R.H. Friend and C. Silva, Appl. Phys. Lett. 94 (2009) 163306.

[19] R. Österbacka, C. P. An, X. M. Jiang, Z.V. Vardeny, Synth. Met. 116 (2001) 317.

[20] J. Piris, T.E. Dykstra, A.A. Bakulin, P.H.M. van Loosdrecht, W. Knulst, M. T. Trinh, J.M. Schins, and L.D.A. Siebbeles, J. Phys. Chem. C 113 (2009)14500

[21] M. Tong, C.-X. Sheng, and Z. V. Vardeny, Phys. Rev. B 75 (2007) 125207， C.-X. Sheng, Z. V. Vardeny, A. B. Dalton, and R. H. Baughman, Phys. Rev. B 71 (2005) 125427

[22] Y. Zhang, G. Hukic-Markosian, D. Mascaro and Z.V. Vardeny, Synth. Metals 160 (2010) 262

[23] X. Wei, Z. V. Vardeny, N. S. Sariciftci, and A. J. Heeger, Phys. Rev. B 53 (1996) 2187

[24]R. Österbacka, X. M. Jiang, C. P. An, B. Horovitz, and Z. V. Vardeny, Phys. Rev. Lett. 88 (2002) 226401

[25] I.A. Howard， R. Mauer, M. Meister,and F. Laquai, J. Am. Chem. Soc. 132 (2010) 14866

[26] T. Drori, C. X. Sheng, A. Ndobe, S. Singh, J. Holt, and Z. V. Vardeny, Phys. Rev. Lett. 101 (2008) 037401.

[27] M. Hallermann, I. Kreigel, E. Da Como, J.M. Berger, E. Von Hauff, and J. Feldmann, Adv. Funct. Mater. 19 (2009) 3662

[28] J. Guo, H. Ohkita, S. Yokoya, H. Benten, and S. Ito, J. Am. Chem. Soc. 132 (2010) 9631

[29]B. Horovitz, Solid State Commun. 41 (1982) 729

[30]E. Ehrenfreund, Z. V. Vardeny, O. Brafman, and B. Horovitz, Phys. Rev. B 36 (1987) 1535

[31] M.J. Rice, Phys. Rev. Lett. 37 (1976) 36

[32] B. Horovitz, H. Gutfreund, and M. Weder, Phys. Rev. B 17 (1978) 2796

[33] P.B. Miranda, D. Moese, and A.J. Heeger, Phys. Rev. B 64 (2001) 081201

[34] C. Silva, A. S. Dhoot, D. M. Russell, M. A. Stevens, A. C. Arias, J. D. MacKenzie, N. C. Greenham, R. H. Friend, S. Setayesh, and K. Müllen, Phys. Rev. B 64(2001) 125211

UU IR Author Manuscript

Captions:

Fig. 1: Cw PA spectrum of RR-P3HT/PCBM blend film at 80 K. Various PA bands are assigned where DP_1 and DP_2 are for delocalized polarons, and P_1 and P_2 are for localized intrachain polarons. The inset shows the DP_1 band in more detail. (b) A model for the energy levels and related allowed optical transitions of intrachain localized polarons and interchain delocalized polarons.

Fig. 2: (a) The transient PM spectrum of RR-P3HT/PCBM blend in the mid-IR range at t=0 ps and 50ps, respectively. The bands PA_1, P_1 and DP_1 are assigned. The inset of (a) is the transient PA spectrum of the same film at t = 0 ps measured after annealing at 150^{o}C for 30 minutes. (b) and (c): Transient dynamics at various PA bands up to 150 ps and 5 ps, respectively. The lines through the data points in (b) are fitting, whereas the lines in (c) are to guide the eye. (d): Excitation intensity dependence of PA_1 dynamics. (e): I–V characteristics under AM 1.5 illumination of P3HT/PCBM photovoltaic device using toluene solution of blends.

Fig. 3: The transient PA spectrum of RR-P3HT/PCBM blend in the near-IR/visible range measured at t=0 ps and 50 ps, respectively. The inset compares the transient dynamics of DP_1 and DP_2 up to 20 ps.

Fig. 4: (a) Transient PA spectrum of RR-P3HT/PCBM blends from 0.13 eV to 0.24 eV measured at t=0 ps, 50 ps, and 200 ps, respectively. Inset of (a) shows the cw PA spectrum in the same spectral range. (b) Transient dynamics at various probe energies.

Fig. 5: Comparison of transient (t= 0 ps) and cw PA spectrum of a pristine RR-P3HT film. (b) Transient dynamics at various probe energies.

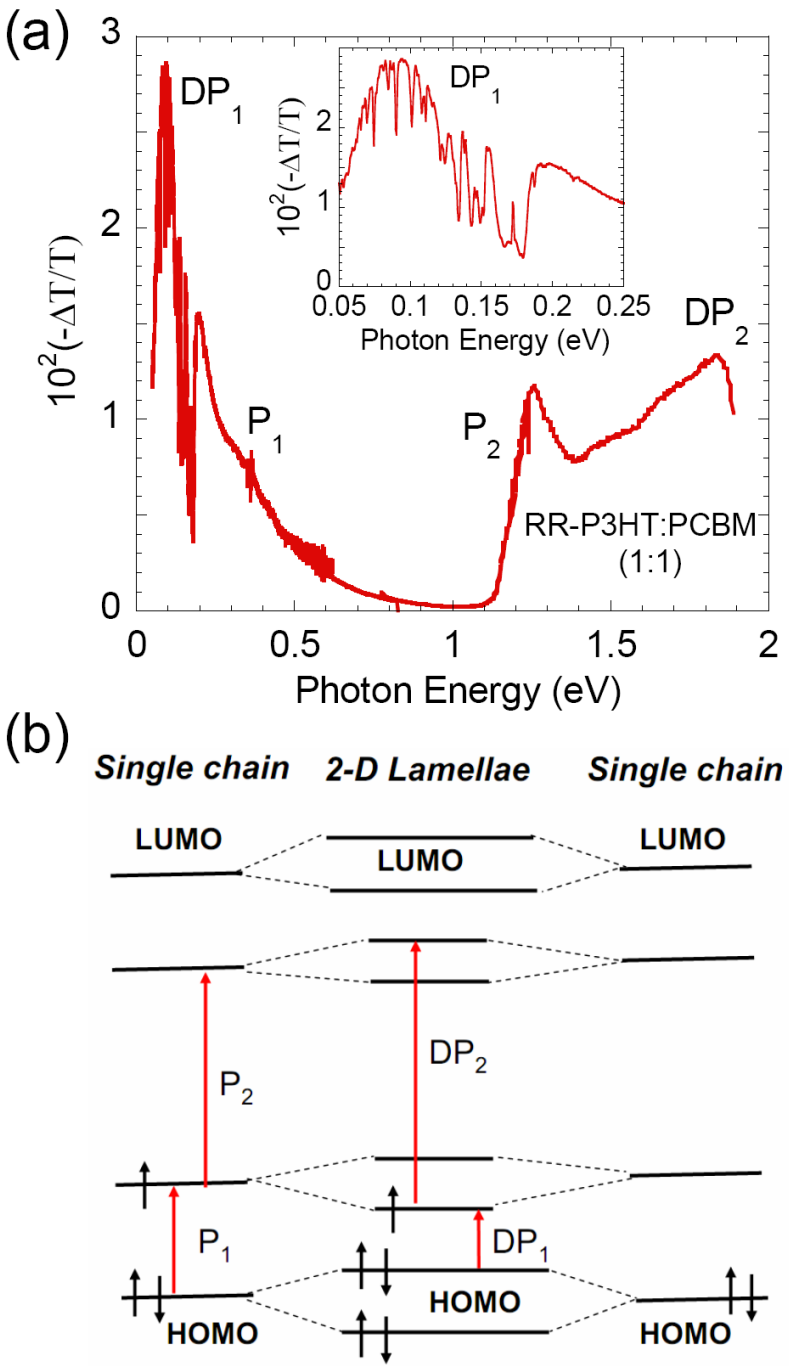

Figure 1

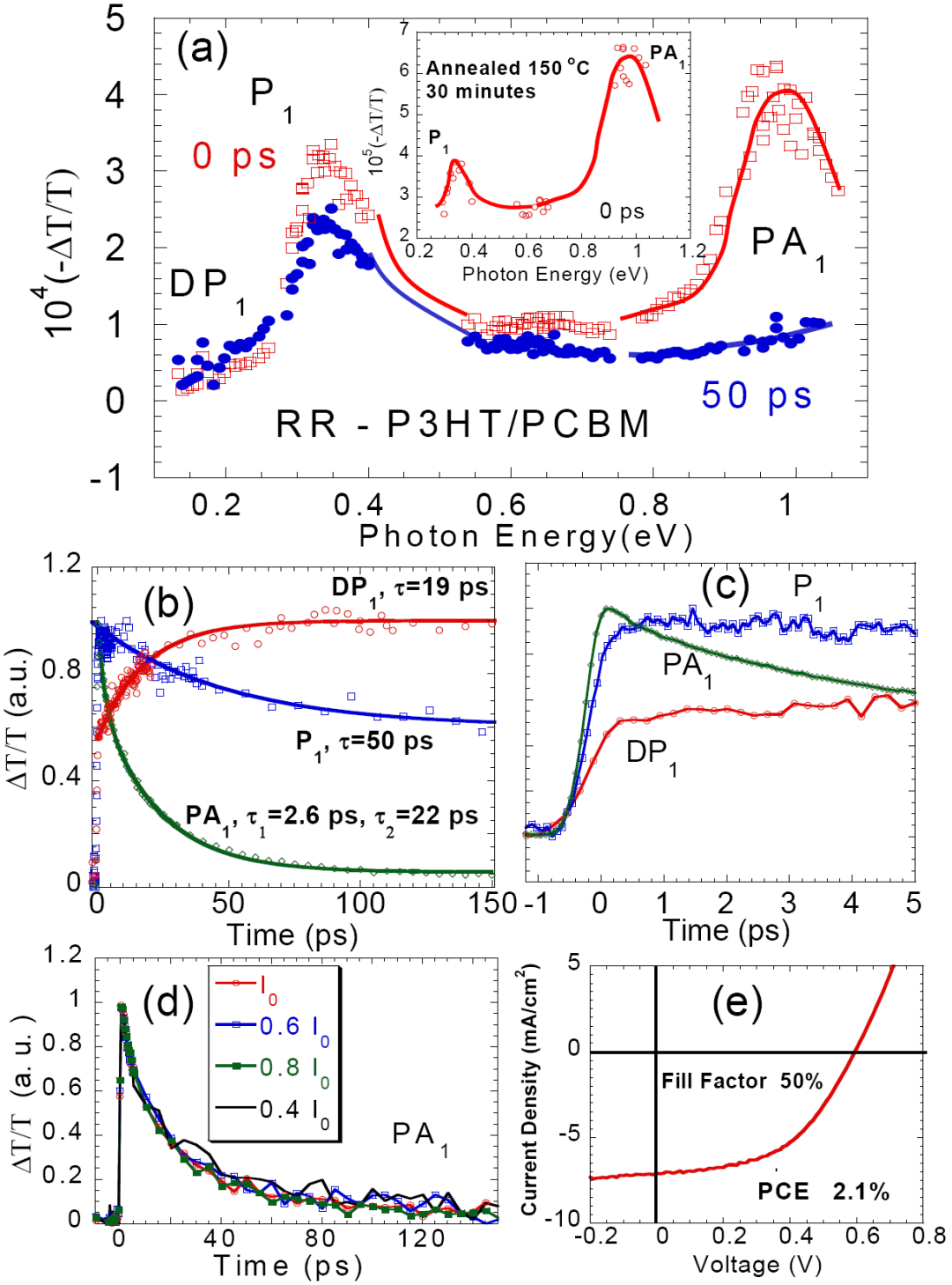

Figure 2

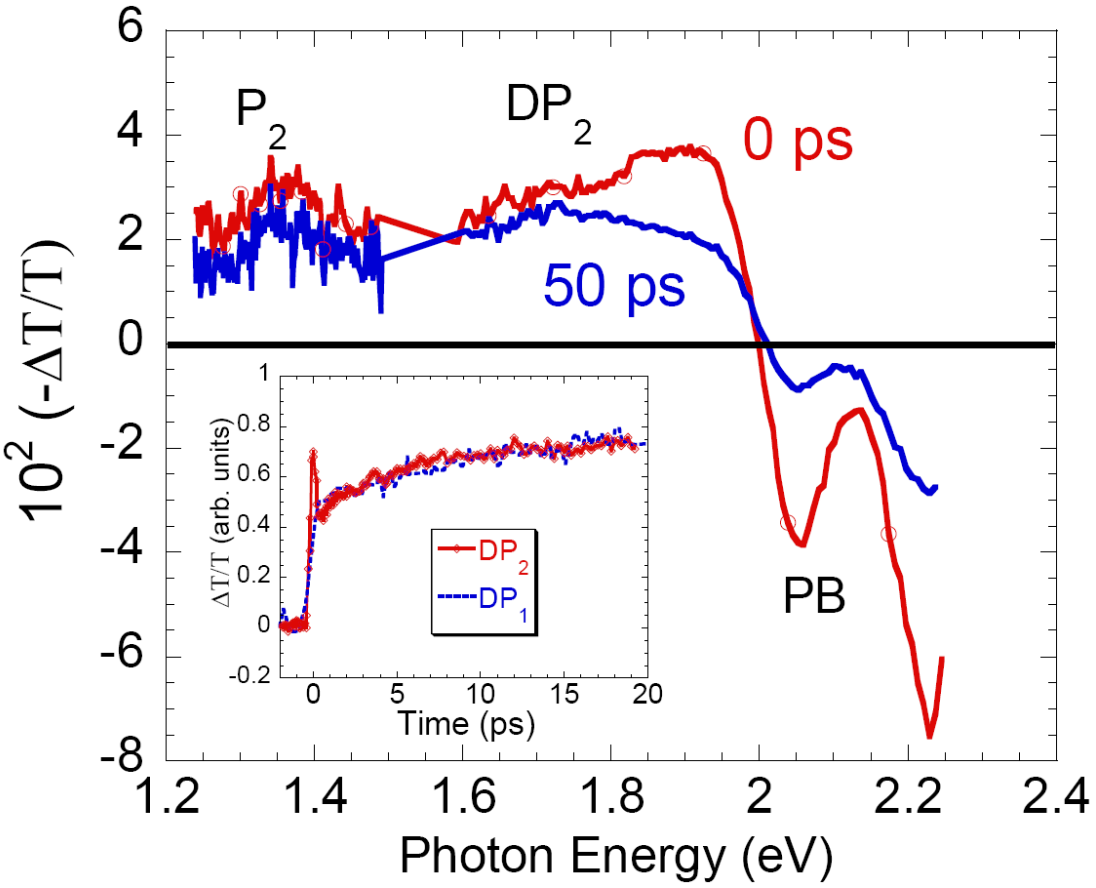

Figure 3

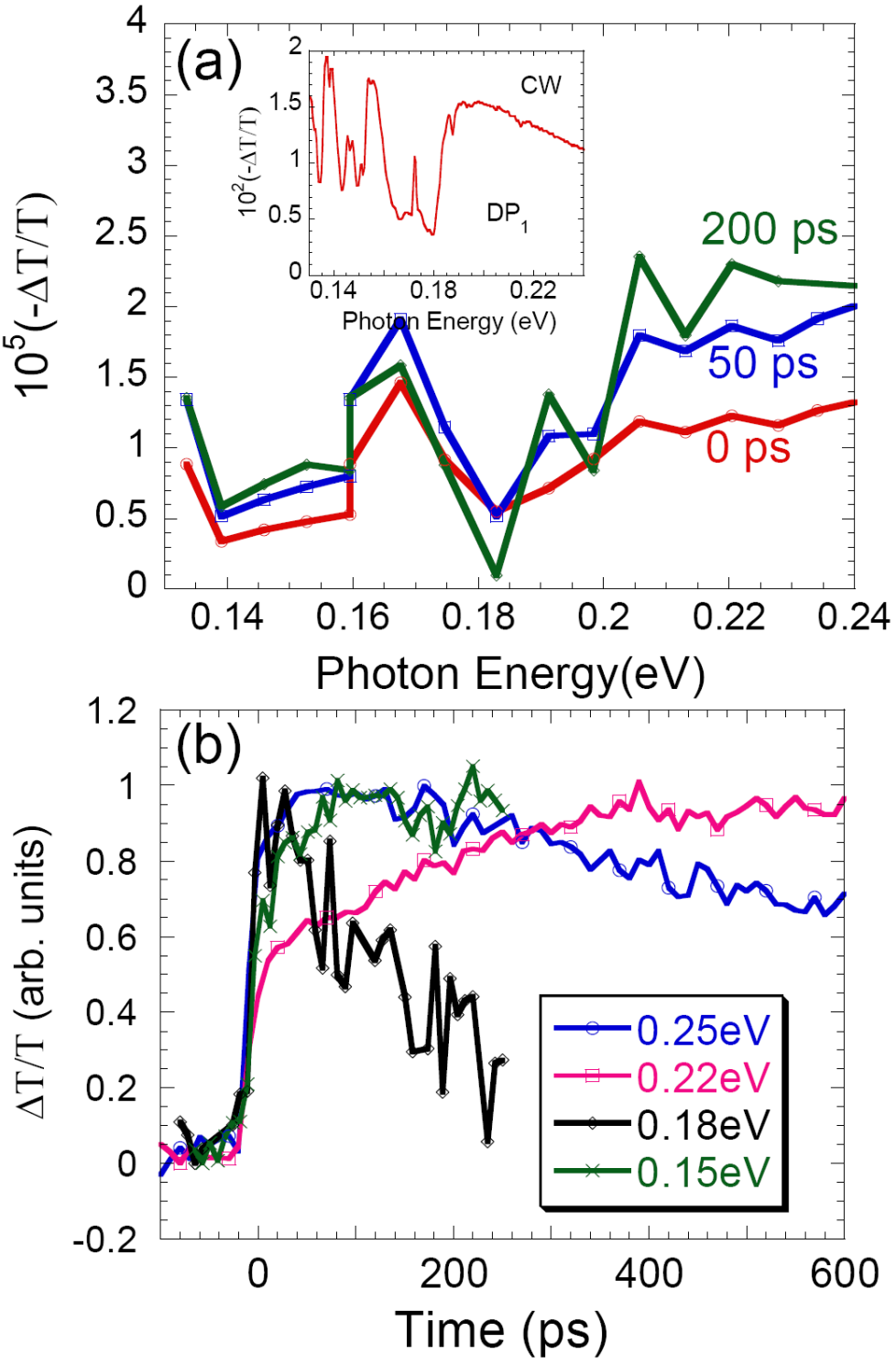

Figure 4

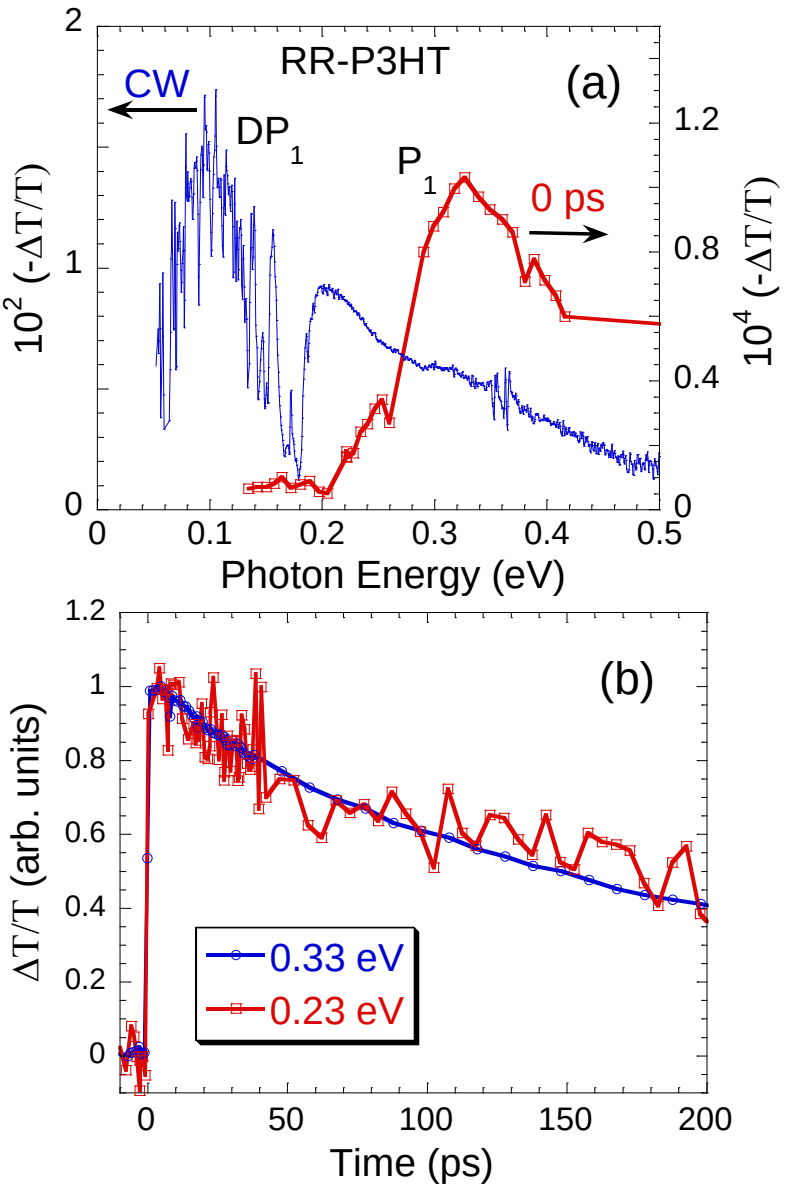

Figure 5

UU IR Author Manuscript